Non-isothermal crystallization kinetics of high density polyethylene/titanium dioxide composites via melt blending

Shichao Wang · Jun Zhang

Abstract In this study, non-isothermal crystallization of neat high density polyethylene (HDPE) and HDPE/titanium dioxide (TiO_2) composite was studied using differential scanning calorimetry. Non-isothermal kinetic parameters were determined by Jeziorny approach and Mo's method. Polarized optical microscopy and wide angle X-ray diffraction were applied to observe the crystal morphology and investigate the crystal structure, respectively. It was found TiO_2 particles could act as nucleating agent during the crystallization process and accelerate the crystallization rate. The Avrami index indicated nucleating type and growth of spherulite of HDPE was relatively simple. The result of activation energy indicated it was more and more difficult for the polymer chains to crystallize into the crystal lattice as the crystallization progressed. HDPE/TiO_2 composites exhibited lower ΔE values, suggesting TiO_2 particle could make the crystallization of HDPE easier. HDPE/TiO_2 composites had much smaller spherulite size than that of neat HDPE. HDPE formed more perfect crystal when TiO_2 particles were added into its matrix without changing the original crystal structure of HDPE.

Keywords Non-isothermal crystallization · High density polyethylene · Titanium dioxide · Composite · Kinetics

Introduction

High density polyethylene (HDPE) is a widely used commercial polymer in industrial field because of its wonderful

S. Wang · J. Zhang (✉)
College of Materials Science and Engineering, Nanjing
University of Technology, Nanjing 210009,
People's Republic of China
e-mail: zhangjun@njut.edu.cn

physical and superior mechanical properties [1]. Inorganic fillers are often added into polymer matrix to improve its mechanical, thermal, optical, magnetic, electrical, surface wear properties [2–4]. Since commercial production of titanium dioxide (TiO_2) appeared in the early twentieth century, it has been widely applied in many fields as gas sensor, white pigment, optical coating, solar cells, etc. [5, 6]. These applications can be divided into "energy" and "environmental" categories, which are largely depended on the perfect properties of TiO_2 itself [6]. In the energy-saving field, it can be used as a passive cooling material due to its exceptional optical properties. First, this wide-gap semiconductor does not absorb either in visible or in the IR regions. Second, TiO_2 has high reflective index 2.57 for anatase and 2.74 for rutile crystal structure, preferable for solar reflectance [7]. Therefore, TiO_2 can be added into HDPE matrix for passive cooling purpose. This kind of material can be fabricated into polymeric shadow net to cover the building roof, tent for rescue, and artificial turf covered on the football playground.

In case of semi-crystalline polymer-like HDPE, the overall properties depend largely on the morphology, the crystalline structure, and the degree of crystallinity [8, 9]. It is significant to understand the kinetic parameters affecting the crystallization process for optimization of the processing condition and the properties of final products [10]. The crystallization process can be carried out under isothermal and non-isothermal crystallization [11]. In general, investigation of isothermal crystallization is idealized, problems related to the cooling rates and thermal gradients within the samples are ignored [12, 13]. Non-isothermal crystallization condition is much closer to the real industrial processing condition [14]. Some researchers evaluate the non-isothermal crystallization process by dividing the process into a sequence of infinitesimally small isothermal stages.

Therefore, the non-isothermal crystallization could be modeled by modification of the Avrami equation [15–17].

Although some literatures have reported the study on HDPE/TiO₂ composite [18–20], studies related with its non-isothermal crystallization are rarely reported in the literatures. Thus, it is reasonable and interesting to determine the non-isothermal crystallization behavior of HDPE/TiO₂ composites. In this study, HDPE was blended with different crystal forms of TiO₂. The non-isothermal crystallization process was characterized by differential scanning calorimetry measurement (DSC). Two equations (Jeziorny theory and Mo's method) were applied to describe the crystallization kinetics. Friedman equation was also used to calculate the effective activation energy. Polarized optical microscopy (POM) and wide angle X-ray diffraction (WAXD) were applied to observe crystal morphology and crystal structure of HDPE, respectively.

Experimental

Materials

High density polyethylene (HDPE 4902T, 0.950 g cm⁻³, 0.225 g/10 min under the pressure of 5 kg at 190 °C) was supplied from Sinopec Yangzi Petrochemical Company Limited, China. Three types of TiO₂ were applied in this investigation. Micro anatase TiO₂ (purity 96.5 %, average particle size 320 nm) was obtained from Nanjing Titanium Company, China. Micro rutile TiO₂ (purity 93.0 %, average particle size 405 nm) was purchased from DuPont Company, USA. Nano mixed crystals TiO₂ (purity 97.8 %, average particle size 20 nm, rutile/anatase = 20/80) was supplied by Evonik Degussa Corporation, Germany.

Preparation of the HDPE/TiO₂ composites

The melt blending of HDPE/TiO₂ was prepared with a torque rheogoniometer (Kechuang machinery XSS-300) at 150 °C and 60 rpm for 6 min. All blends were added with 3 mass% loading of TiO₂.

DSC measurements

Non-isothermal crystallization of all samples were conducted with DSC using a Q200 thermal analysis apparatus (TA Instruments, America). For measurement, samples (∼10 mg) were cut off and sealed into aluminum pans. To prevent thermal degradation of all samples, dry nitrogen gas was applied with a flux of 50 mL min⁻¹ during the scanning. All samples were heated from room temperature to 165 °C at a rate of 40 °C min⁻¹, and maintained at this temperature for 2 min to eliminate the former thermal

history. The non-isothermal crystallization process of composites was run at a series of cooling rates (2.5, 5, 10, 20 °C min⁻¹) to obtain the crystallization curves from 165 to 40 °C, respectively. The crystallinity X_{DSC} was calculated by the following equation:

$$X_{DSC} = [\Delta H / (\Delta H_f^* \cdot \phi)] \times 100\% \tag{1}$$

where ΔH was enthalpy of each sample measured by DSC, $\Delta H_f^* = 277.1$ J g⁻¹ is the melting enthalpy of fusion for a 100 % crystalline of polyethylene (PE), ϕ is the mass fraction of HDPE in the composites. The half-time crystallization ($t_{1/2}$) calculated from the DSC curve was used to characterize the crystallization process.

Polarized optical microscopy (POM) observation

To observe the crystal morphology, polarized microscopy was applied under polarized light in the dark background using a polarizing microscope (Olympus BX 51, Japan) equipped with a temperature controller (Linkam THMS 600, England). Extremely thin sample slices (ca. 0.02 mm) were heated up to 165 °C, and were held on this temperature for 3 min to eliminate all the thermal history. Then, samples were cooled to the room temperature at a slow rate of 5 °C min⁻¹. Photograph of full-grown spherulite was taken when the crystallization was completely accomplished.

Wide angle X-ray diffraction (WAXD) analysis

The crystal structure was investigated by XRD-6000 diffractometer (Shimadzu, Japan) using nickel-filtered Cu Kα source. The scanning velocity was 5° min⁻¹ ranging from 10 to 60° at a voltage of 40 kV and a filament current of 30 mA under ambient temperature. The interplanar distance (d value) and crystal thickness L were calculated using Bragg equation and Scherrer equation, respectively. The overall degree of the crystallinity was measured as reported in literature [21].

Results and discussion

Non-isothermal crystallization behavior

Figure 1 shows the crystallization curves for neat HDPE and HDPE/TiO₂ composites at four different cooling rates (2.5, 5, 10, 20 °C min⁻¹). As shown in Fig. 1, all samples display the same tendency: the crystallization peaks shift to lower temperature as the cooling rate increases. Moreover, the faster the cooling rate is, the lower the crystallization temperature occurs. This indicates that fast cooling rate has a retardation effect on the nucleation and crystal growth

[22–24]. Some kinetic parameters obtained from the DSC curves are listed in Table 1. At a given cooling rate, it is suggested that HDPE had lower onset crystallization temperature (T_c^{on}), crystallization enthalpy (ΔH_c), and broader temperature range than those of all HDPE/TiO$_2$ composites. These suggest the addition of TiO$_2$ particles accelerate the crystallization rate remarkably, and TiO$_2$ could lead to more perfect crystallization than the neat HDPE. The half-time crystallization $t_{1/2}$ decreases when TiO$_2$ particles are added into the HDPE matrix. At this low content, TiO$_2$ can act as nucleating agent during the non-isothermal crystallization process, therefore accelerate the crystallization [25]. The crystallization enthalpy (ΔH_c) appears a maximum value when the cooling rate is 5 °C min^{-1}. This cooling rate is regarded as the optimal crystallization rate for nucleation and lamellae growth. There is insufficient time for nucleation at higher crystallization rate. Polymer chains are lack of driving force for lamellae growth at lower crystallization rate [21]. All TiO$_2$ particles have the lower values of half-time crystallization in comparison with neat HDPE indicating they have the best nucleation effect on the HDPE matrix and accelerate the crystallization rate most obviously [25].

Based on the Avrami equation, the relative degree of crystallinity (X_t) as a function of temperature (T) and time

Table 1 Crystallization parameters obtained from DSC curves directly at various cooling rates and non-isothermal crystallization kinetic parameters determined from Jeziorny theory

Samples	$D/$ °C min^{-1}	$T_c^{on}/$ °C	$\Delta H_c/$ J g^{-1}	$t_{1/2}/$ s	n	Z_t	Z_c
HDPE	2.5	120.6	187.1	63.8	2.3	0.7	0.9
	5	119.5	192.2	44.5	2.2	1.7	1.1
	10	118.2	182.3	30.6	2.0	3.1	1.1
	20	116.5	173.5	22.9	2.0	5.7	1.1
HDPE/anatase	2.5	121.0	196.0	50.3	2.2	1.0	1.0
	5	119.9	202.0	31.3	1.8	2.5	1.2
	10	118.7	191.6	20.5	1.6	4.1	1.2
	20	117.1	182.2	14.5	1.4	5.6	1.1
HDPE/rutile	2.5	121.1	197.7	51.1	2.2	1.0	1.0
	5	120.4	204.0	32.1	2.2	3.2	1.3
	10	118.8	195.1	21.7	1.9	4.7	1.2
	20	117.3	185.4	15.8	1.7	6.6	1.1
HDPE/mixed crystals	2.5	120.9	190.9	50.8	2.1	1.1	1.0
	5	119.9	198.4	32.1	1.9	2.5	1.2
	10	118.7	190.1	21.3	1.6	4.2	1.2
	20	117.2	182.2	15.7	1.6	6.4	1.1

D cooling rate, T_c^{on} onset crystallization temperature, ΔH_c crystallization enthalpy

Fig. 1 DSC cooling curves of neat HDPE and HDPE/TiO$_2$ composites during non-isothermal crystallization at different cooling rates
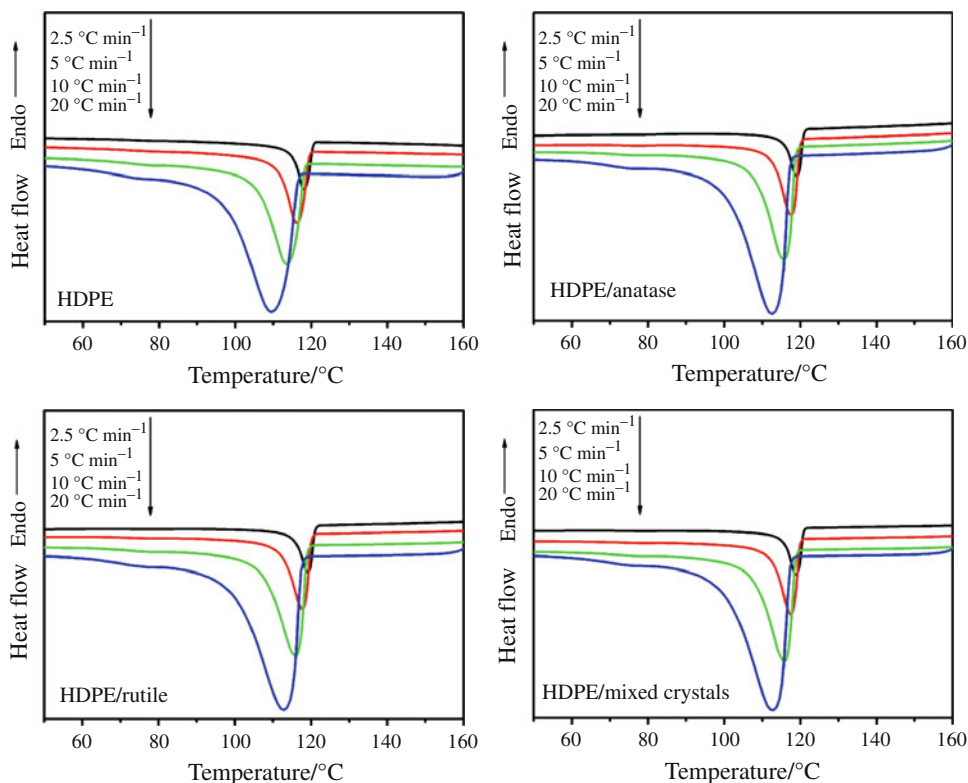
(t) can be calculated as the ratio of the areas of crystallization peak as following form:

$$X_t = \left[\int_{T_0}^{T} (dH_c/dT) \times dT \right] \Bigg/ \left[\int_{T_0}^{T_\infty} (dH_c/dT) \times dT \right] \quad (2)$$

where T_0 and T are the initial and final crystallization temperature at time t, respectively. dH_c is the enthalpy of crystallization released during an infinitesimal temperature interval. In the non-isothermal crystallization process, crystallization time t can be calculated by the following formulation, in which D refers to the cooling rate

$$t = |T - T_0|/D \quad (3)$$

The plots of relative X_t against crystallization time t for neat HDPE and HDPE/TiO$_2$ composites are shown in Fig. 2. Because nucleation occurs from the melt and slows down as the crystallization progresses, all curves display approximately the S shape [25]. All curves end up with a flat line because of the spherulite impingement. As cooling rate increases, the time for crystallization accomplishment becomes shorter and shorter [26, 27].

Jeziorny theory

The widely used Avrami equation for isothermal crystallization was described as follows [12]:

$$1 - X_t = \exp(-Z_t t^n) \quad (4)$$

where Z_t represents the crystallization rate constant; n is an Avrami index containing information about the nucleation mechanism and crystal growth dimension. Based on the assumption that the crystallization temperature is constant, using the double-logarithmic form of Eq. (4), the function is given as follows:

$$\log[-\ln(1 - X_t)] = \log Z_t + n \log t \quad (5)$$

By plotting $\log[-\ln(1 - X_t)]$ versus $\log t$ for each cooling rate, all data can be fitted into a straight line, from which Z_t and n can be calculated as the intercept and slope, respectively. Considering the practical non-isothermal crystallization circumstance, Jeziorny suggested that the parameter, Z_t, should be corrected as follows [28]:

$$\log Z_c = \log Z_t/D \quad (6)$$

Figure 3 shows the plots of $\log[-\ln(1 - X_t)]$ against $\log t$. Each curve shows a good linear relationship and shifts to shorter time with the increasing cooling rate. All fitting lines are approximately parallel to each other indicating the crystallization mechanism and crystal growth geometries of samples are similar to each other [23]. Kinetic parameters determined by Jeziorny theory are summarized in Table 1. The value of n is dependent on the crystallization mechanisms [29]. In other polymer system, the n value was larger than 4, because of its complicated nucleation type and growth form of spherulite [21, 23, 30]. This phenomenon is not observed in this study indicating nucleating type and growth of spherulite of HDPE is

Fig. 2 The degree of crystallinity versus time of neat HDPE and HDPE/TiO$_2$ composites
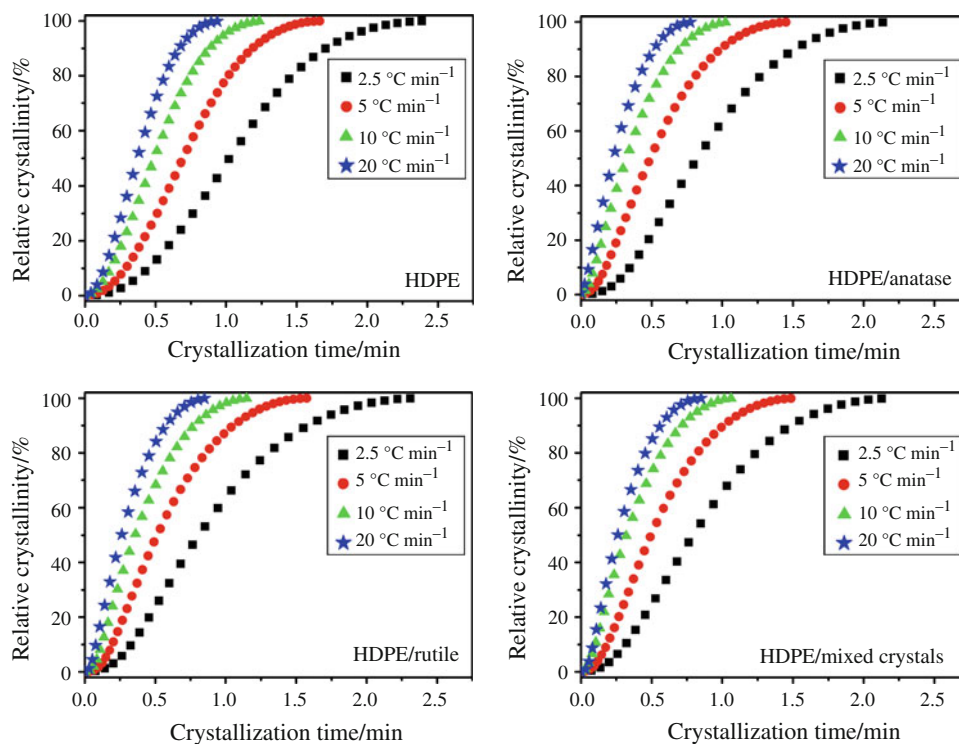
relatively simple [1]. All samples exhibit almost the same value of n, suggesting that TiO$_2$ particles had no effect on the crystallization mechanism of HDPE. Z_c values represent the crystallization rate [21]. Considering the heterogeneous nucleation effect of TiO$_2$, Z_c value of HDPE/TiO$_2$ composites is, as expected, a little higher than neat HDPE, indicating TiO$_2$ particles favor the overall crystallization process. This result is in accordance with the result of half crystallization time ($t_{1/2}$). It is found the linear trend is lost in the latter stage of crystallization. In some researches [21, 31], the Jeziorny curves were divided into two linear sections (the primary and the second crystallization stage). In this study, latter nonlinear stage is due to the secondary crystallization, but it proceeds at a much slower rate after the impingement of adjacent spherulites. Phenomenon above was observed prevalently in literatures [14, 30].

Mo's method

In order to describe the non-isothermal crystallization process more precisely, Mo and coworkers [8, 17] have proposed a convenient method by combining the expanded Avrami equation and the Ozawa [28] equation:

$$\log D = \log F_T - \alpha \log t \qquad (7)$$

in which, $F_T = [K_T/Z_t]^{1/m}$ stands for the value of cooling rate chosen at unit crystallization time when the measured system amounts to a defined degree of crystallinity, $\alpha = n/m$ is the ratio of Avrami exponent n to the Ozawa exponent m. Figure 4 illustrates the plotting of log D against log t. As can be seen, there is a good linear relationship between log D and log t.

Values of F_T and α calculated from the intercept and slope of the plots are listed in Table 2. Values of F_T and α increase gradually with the increase of relative crystallinity, indicating the crystallization becomes more difficult as the crystallization progresses. In comparison with the neat HDPE, HDPE/TiO$_2$ composites have lower values of F_T. F_T is related to the cooling rate needed to reach a given crystallinity in a unit time [32]. From this point of view, HDPE/TiO$_2$ composites have higher crystallization rate than that of neat HDPE. In other words, TiO$_2$ acts as a nucleating agent during the crystallization stage therefore it enhances the overall crystallization rate. All the results indicate that Mo's analysis is suitable to investigate the non-isothermal crystallization process in this study.

Crystallization activation energy

Methods mentioned above have not been proposed for calculating activation energy (ΔE) for the non-isothermal crystallization process. Kissinger, Vyazovkin, and Friedman [33, 34] put forward different mathematical model to evaluate the ΔE value. In this article, the differential iso-conversional mathematical method of Friedman is applied to estimate activation energy. Activation energy is calculated for every degree of crystallinity from [35]:

Fig. 3 Plots of log($-\ln(1 - X_t)$) versus log t for non-isothermal crystallization of neat HDPE and HDPE/TiO$_2$ composites
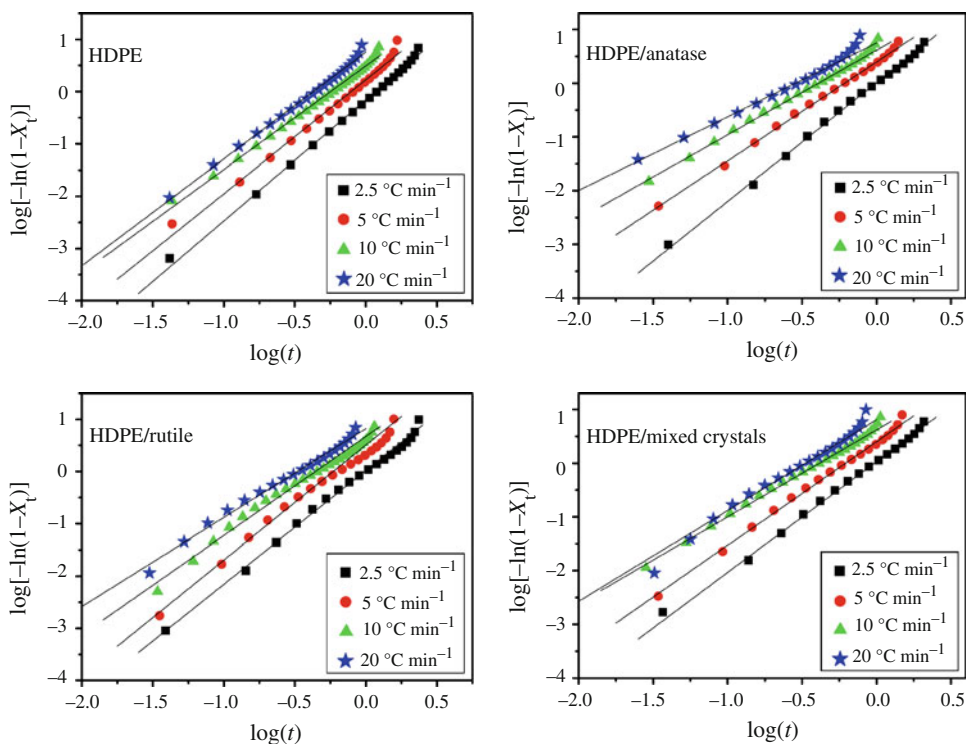
Fig. 4 Plots of log D versus log t from the Mo's method for non-isothermal crystallization of neat HDPE and HDPE/TiO$_2$ composites
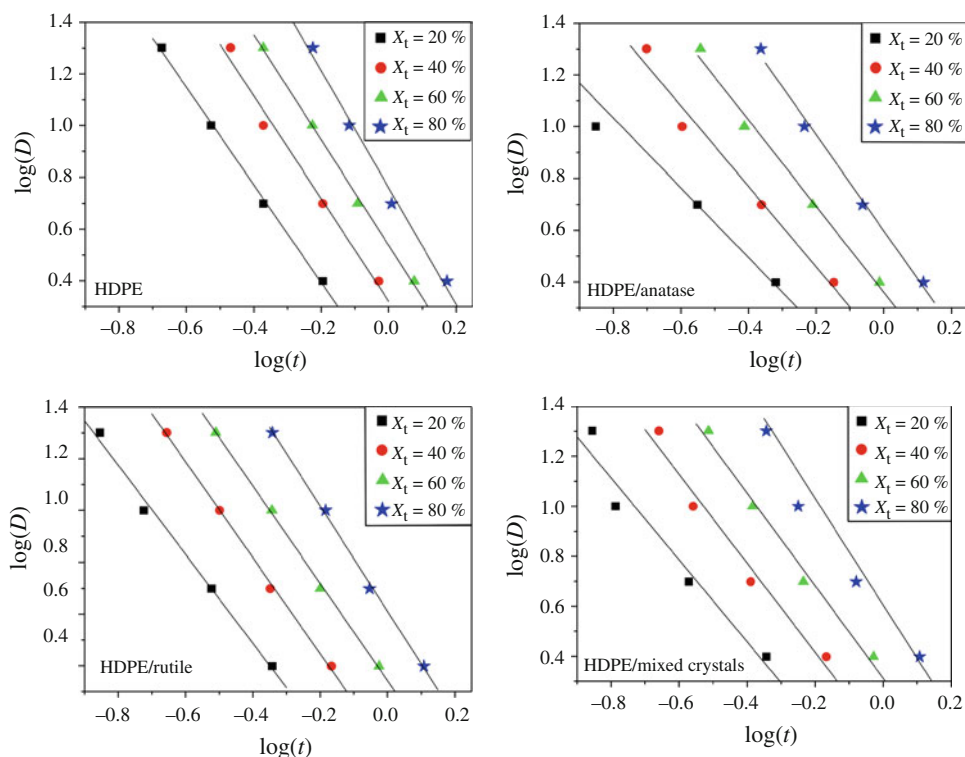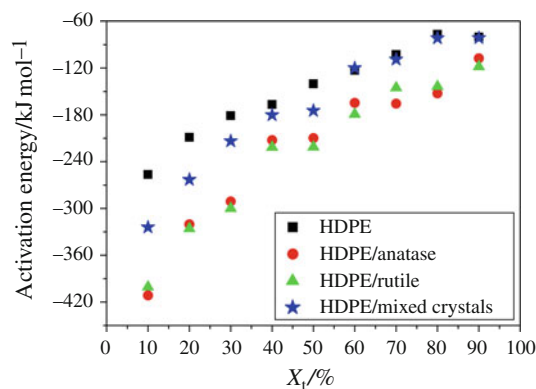

Table 2 Non-isothermal crystallization kinetic parameters obtained from Mo's method

Samples	X_t/%	20	40	60	80
HDPE	F_T	1.03	2.09	3.44	5.75
	a	1.89	1.99	2.04	2.26
HDPE/anatase	F_T	0.90	1.41	2.29	3.96
	a	1.35	1.55	1.66	1.85
HDPE/rutile	F_T	0.63	1.19	2.20	4.08
	a	1.72	1.86	1.88	2.03
HDPE/mixed crystals	F_T	0.63	1.15	2.05	3.77
	a	1.64	1.78	1.85	1.94

Fig. 5 Non-isothermal crystallization activation energy of neat HDPE and HDPE/TiO$_2$ composites

$$\ln(dX_t/dt)_{X_t} = C - \Delta E/(R \cdot T) \tag{8}$$

where C is an arbitrary pre-exponential factor, ΔE stands for activation energy at a given relative crystallinity X_t. R is the universal gas constant (8.314 J mol^{-1} K^{-1}). T refers to a series of temperatures related to a given crystallinity X_t at different cooling rates D. dX_t/dt is the instantaneous crystallization rate as a function of time at a given relative crystallinity X_t. The correlated crystallization temperature T at a specific X can be chosen by selecting appropriate relative degrees of crystallinity (i.e., 10–90 %). By plotting the $\ln (dX_t/dt)_{X_t}$ against $1/T$, the crystallization activation energy ΔE can be calculated from the slope of the straight line. The activation energy ΔE versus the relative degree of crystallinity is plotted in Fig. 5.

The ΔE values increases with the increase in the relative degrees of crystallinity for neat HDPE and HDPE/TiO$_2$ composites. These results suggest that it was more difficult to crystallize as the crystallization progresses [30, 36]. It is interesting to find that HDPE/TiO$_2$ composites exhibits lower ΔE values, suggesting TiO$_2$ particle could make the crystallization of HDPE easier [10]. This could also be verified by the results of the half crystallization time ($t_{1/2}$). TiO$_2$ accelerates the crystallization process of HDPE acting as a nucleating agent [37]. HDPE blended with anatase TiO$_2$ has the lowest value of ΔE, which indicates that anatase TiO$_2$ is the most nucleating agent of HDPE matrix. As the relative degree of crystallinity increased to 90 %, all samples show similar ΔE values. The crystallization

process can be divided into nucleation and crystal growth stages. TiO$_2$ particle acts as the nucleating agents to make the initial stage of crystallization easier. However, TiO$_2$ has less effect in the crystal stage when the formation of nuclei is completed. Therefore, TiO$_2$ has no superior in the crystallization at the last crystallization stage.

Crystal morphology based on POM analysis The crystal morphology is shown in Fig. 6. The neat HDPE exhibits larger spherulite size than in HDPE/TiO$_2$ composites. This can be judged by the amount of light spots in the field of view. Compared with the neat HDPE, HDPE/TiO$_2$ composites have higher density of nuclei, and smaller spherulite size. The larger number of nuclei might originate from TiO$_2$ particles in the polymer matrix, indicating that the TiO$_2$ has a nucleating effect on HDPE matrix. After the formation of nuclei, the crystal trend to grow on these nuclei to form smaller spherulites [38]. Similar morphology behavior was observed in other HDPE systems [37–39]. The crystal morphology is also in accordance with the conclusion deduced by DSC measurement.

Crystal structure based on WAXD analysis The WAXD is conducted to investigate the crystal structure of neat HDPE and HDPE/TiO$_2$ composites. In Fig. 7, two obvious diffractive peaks about 22.0°, 22.4° are corresponding to typical crystal plane (110), (200) of orthorhombic phase, respectively [16]. The interplanar distance (*d* value) represents lattice parameters [40], which proves that lattice

parameter is not affected by TiO$_2$ particles (Table 3). Moreover, the diffractive peaks do not shift with the addition of TiO$_2$. This clearly indicates the unchanged crystal structure of HDPE, i.e., addition of TiO$_2$ did not exert an effect on the crystalline structure of the HDPE, suggesting the occurrence of no molecular level interaction [16]. Lamellar thickness (*L*) increases with the addition of TiO$_2$ particles, implying TiO$_2$ leads the formation of more perfect crystals. This behavior can be related to the non-isothermal crystallization model discussed previously. This can be attributed to the fact that TiO$_2$ particles act as the heterogeneous nucleating agent inducing HDPE to form some perfect and stable crystals. The degree of crystallinity
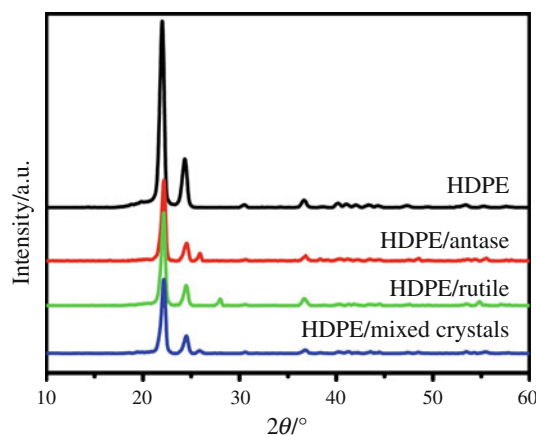

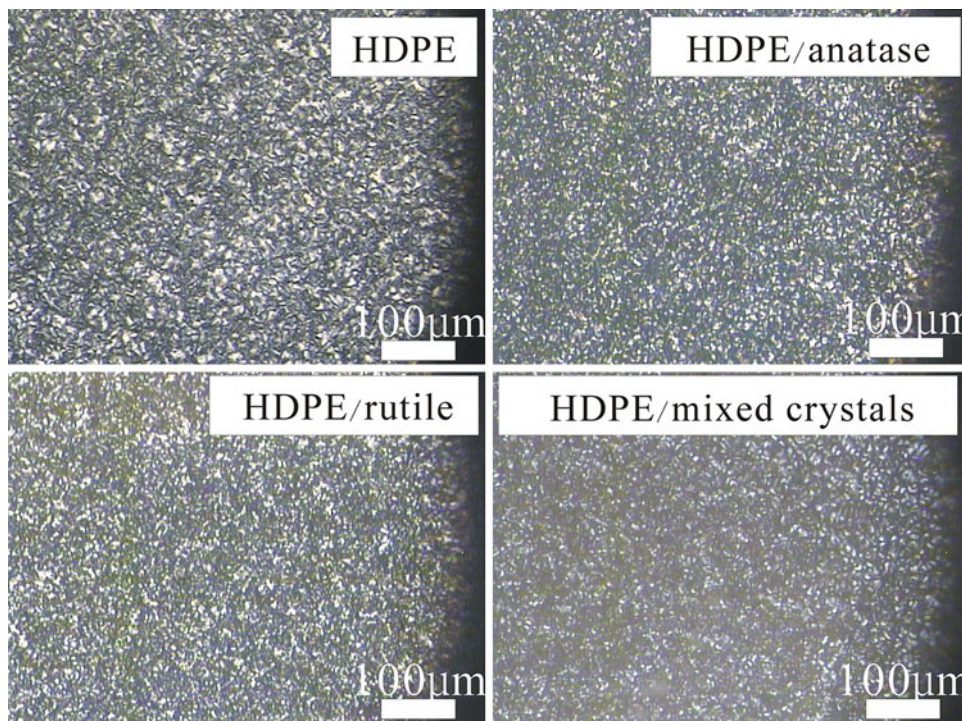**Fig. 7** WAXD patterns of HDPE and HDPE/TiO$_2$ composites

Fig. 6 Crystal morphology of neat HDPE and HDPE/TiO$_2$ composites

Table 3 WAXD parameters of neat HDPE and HDPE/TiO$_2$ composites

Samples	hkl	2θ/°	d/Å	L/Å	The degree of crystallinity/%	
					X_{DSC}	X_{WAXD}
HDPE	110	22.0	4.0	166.9	61.6	83.0
	200	24.3	3.7	152.0		
HDPE/anatase	110	22.1	4.0	194.5	56.3	64.0
	200	24.5	3.6	162.9		
HDPE/rutile	110	22.1	4.0	195.4	57.4	57.7
	200	24.5	3.6	174.7		
HDPE/mixed crystals	110	22.1	4.0	186.2	54.0	60.4
	200	24.5	3.6	168.2		

of HDPE measured by DSC (X_{DSC}) and WAXD (X_{WAXD}) are also listed in Table 3. The degree of crystallinity calculated by WAXD shows the same tendency with the result determined by DSC. However, X_{WAXD} is a little higher than X_{DSC}. This may be attributed to the technique of measurement. Some amorphous parts might be calculated into the crystal region by WAXD measurement. TiO$_2$ particle causes a decrease in the degree of crystallinity, demonstrating that TiO$_2$ has a hindering effect on the degree of crystallinity. Some previous researchers have already reported the inorganic fillers suppressed the degree of crystallinity [41, 42].

Conclusions

In this research, DSC is carried out to investigate the non-isothermal crystallization kinetics of HDPE and HDPE/TiO$_2$ composites. TiO$_2$ accelerates the crystallization rate and has a nucleation effect on HDPE. The most suitable rate is 5 °C min^{-1} for the crystallization of HDPE matrix. Both Jeziorny and Mo's method are able to profile the non-isothermal crystallization kinetics of HDPE and HDPE/TiO$_2$ composites satisfactorily. Both Jeziorny and Mo's method exhibit that the TiO$_2$ particle acts as a nucleation agent in HDPE matrix and enhances the overall crystallization rate. Anatase TiO$_2$ accelerates the crystallization rate most obviously, and rutile TiO$_2$ has the best nucleation effect. The result of activation energy indicates that it becomes more and more difficult for the polymer chains to crystallize into crystal lattice as the crystallization progresses. TiO$_2$ particle makes the crystallization an easier process of HDPE with lower activation energy. The POM analysis also proves that TiO$_2$ promotes the crystallization by acting as the nucleating agent. HDPE formed more perfect crystal when TiO$_2$ particles were added into its matrix without changing the original crystal structure of HDPE.

References

1. Zou P, Tang SW, Fu ZZ, Xiong HG. Isothermal and non-isothermal crystallization kinetics of modified rape straw flour/high-density polyethylene composites. Int J Therm Sci. 2009;48(4):837–46.
2. Jung J, Kim J, Uhm YR, Jeon J-K, Lee S, Lee HM, et al. Preparations and thermal properties of micro- and nano-BN dispersed HDPE composites. Thermochim Acta. 2010;499(1–2):8–14.
3. Chrissafis K, Paraskevopoulos KM, Pavlidou E, Bikiaris D. Thermal degradation mechanism of HDPE nanocomposites containing fumed silica nanoparticles. Thermochim Acta. 2009;485(1–2):65–71.
4. Alexandre M, Dubois P. Polymer-layered silicate nanocomposites: preparation, properties and uses of a new class of materials. Mat Sci Eng R. 2000;28(1–2):1–63.
5. Brandt K, Salikov V, Oezcoban H, Staron P, Schreyer A, Prado LASA, et al. Novel ceramic-polymer composites synthesized by compaction of polymer-encapsulated TiO$_2$-nanoparticles. Compos Sci Technol. 2011;72(1):65–71.
6. Chen X, Mao SS. Titanium dioxide nanomaterials: synthesis, properties, modifications, and applications. Chem Rev. 2007;107(7):2891–959.
7. Mastai Y, Diamant Y, Aruna ST, Zaban A. TiO2 nanocrystalline pigmented polyethylene foils for radiative cooling applications: synthesis and characterization. Langmuir. 2001;17(Compendex):7118–23.
8. Li J, Fang Z, Tong L, Gu A, Liu F. Effect of multi-walled carbon nanotubes on non-isothermal crystallization kinetics of polyamide 6. Eur Polym J. 2006;42(12):3230–5.
9. Weng WG, Chen GH, Wu DJ. Crystallization kinetics and melting behaviors of nylon 6/foliated graphite nanocomposites. Polymer. 2003;44(26):8119–32.
10. Vassiliou AA, Papageorgiou GZ, Achilias DS, Bikiaris DN. Nonisothermal crystallisation kinetics of in situ prepared poly(epsilon-caprolactone)/surface-treated SiO$_2$ nanocomposites. Macromol Chem Phys. 2007;208(4):364–76.
11. Jeziorny A. Parameters characterizing kinetics of nonisothermal crystallizaiton of poly (ethylene-terephthalate) determined by DSC. Polymer. 1978;19(10):1142–4.
12. Di Lorenzo ML, Silvestre C. Non-isothermal crystallization of polymers. Prog Polym Sci. 1999;24(6):917–50.
13. Qian J, He P. Non-isothermal crystallization of HDPE/nano-SiO$_2$ composite. J Mater Sci. 2003;38(Compendex):2299–304.
14. Chen X, Wang L, Liu Y, Shi J, Shi H. Nonisothermal crystallization kinetics of high-density polyethylene/barium sulfate nanocomposites. Polym Eng Sci. 2009;49(12):2342–9.
15. Papageorgiou GZ, Bikiaris DN, Achilias DS. Effect of molecular weight on the cold-crystallization of biodegradable poly(ethylene succinate). Thermochim Acta. 2007;457(1–2):41–54.
16. Jayasree TK, Predeep P. Non-isothermal crystallization behavior of styrene butadiene rubber/high density polyethylene binary blends. J Therm Anal Calorim. 2012;108(3):1151–60.
17. Alvarez VA, Pérez CJ. Effect of different inorganic filler over isothermal and non-isothermal crystallization of polypropylene homopolymer. J Therm Anal Calorim. 2012;107(2):633–43.
18. Hashimoto M, Takadama H, Mizuno M, Kokubo T. Mechanical properties and apatite forming ability of TiO$_2$ nanoparticles/high density polyethylene composite: effect of filler content. J Mater Sci Mater M. 2007;18(4):661–8.

19. Kasanen J, Suvanto M, Pakkanen TT. Improved adhesion of TiO₂-based multilayer coating on HDPE and characterization of photocatalysis. J Appl Polym Sci. 2011;119(4):2235–45.

20. Takadama H, Hashimoto M, Takigawa Y, Mizuno M, Kokubo T. Effect of melt flow rate of polyethylene on bioactivity and mechanical properties of polyethylene/titania composites. Bioceramics. 2004;16(245–2):569–72.

21. Chen S, Jin J, Zhang J. Non-isothermal crystallization behaviors of poly(4-methyl-pentene-1). J Therm Anal Calorim. 2011;103(1):229–36.

22. Liu XH, Wu QJ. Non-isothermal crystallization behaviors of polyamide 6/clay nanocomposites. Eur Polym J. 2002;38(7):1383–9.

23. Zhang J, Chen S, Su J, Shi X, Jin J, Wang X, et al. Non-isothermal crystallization kinetics and melting behavior of EAA with different acrylic acid content. J Therm Anal Calorim. 2009;97(3):959–67.

24. Huang YP, Chen GM, Yao Z, Li HW, Wu Y. Non-isothermal crystallization behavior of polypropylene with nucleating agents and nano-calcium carbonate. Eur Polym J. 2005;41(11):2753–60.

25. Peng Z, Kong LX, Li SD. Non-isothermal crystallisation kinetics of self-assembled polyvinylalcohol/silica nano-composite. Polymer. 2005;46(6):1949–55.

26. Jain S, Goossens H, van Duin M, Lemstra P. Effect of in situ prepared silica nano-particles on non-isothermal crystallization of polypropylene. Polymer. 2005;46(20):8805–18.

27. Kim JY, Park HS, Kim SH. Unique nucleation of multi-walled carbon nanotube and poly(ethylene 2,6-naphthalate) nanocomposites during non-isothermal crystallization. Polymer. 2006;47(4):1379–89.

28. Saengsuwan S, Tongkasee P, Sudyoadsuk T, Promarak V, Keawin T, Jungsuttiwong S. Non-isothermal crystallization kinetics and thermal stability of the in situ reinforcing composite films based on thermotropic liquid crystalline polymer and polypropylene. J Therm Anal Calorim. 2011;103(3):1017–26.

29. Wang JB, Dou Q. Non-isothermal crystallization kinetics and morphology of isotactic polypropylene (iPP) nucleated with rosin-based nucleating agents. J Macromol Sci B. 2007;46(5):987–1001.

30. Zhang J, Chen S, Jin J, Shi X, Wang X, Xu Z. Non-isothermal melt crystallization kinetics for ethylene-acrylic acid copolymer in diluents via thermally induced phase separation. J Therm Anal Calorim. 2010;101(1):243–54.

31. Jin J, Chen SJ, Zhang J. Non-isothermal crystallization kinetics of partially miscible ethylene-vinyl acetate copolymer/low density polyethylene blends. Express Polym Lett. 2010;4(3):141–52.

32. Qin JL, Li ZT. Nonisothermal crystallization, melting behavior, and morphology of PP/EPPE blends. J Appl Polym Sci. 2010;115(2):1256–63.

33. Huang H, Gu LX, Ozaki Y. Non-isothermal crystallization and thermal transitions of a biodegradable, partially hydrolyzed poly(vinyl alcohol). Polymer. 2006;47(11):3935–45.

34. Apiwanthanakorn N, Supaphol P, Nithitanakul M. Non-isothermal melt-crystallization kinetics of poly(trimethylene terephthalate). Polym Test. 2004;23(7):817–26.

35. Achilias DS, Papageorgiou GZ, Karayannidis GR. Evaluation of the isoconversional approach to estimating the Hoffman-Lauritzen parameters from the overall rates of non-isothermal crystallization of polymers. Macromol Chem Phy. 2005;206(15):1511–9.

36. Qin JL, Guo SQ, Li ZT. Melting behavior and isothermal crystallization kinetics of PP/mLLDPE blends. J Polym Res. 2008;15(5):413–20.

37. Huang JW, Wen YL, Kang CC, Tseng WJ, Yeh MY. Nonisothermal crystallization of high density polyethylene and nanoscale calcium carbonate composites. Polym Eng Sci. 2008;48(7):1268–78.

38. Song S, Wu P, Ye M, Feng J, Yang Y. Effect of small amount of ultra high molecular weight component on the crystallization behaviors of bimodal high density polyethylene. Polymer. 2008;49(12):2964–73.

39. Kim J, Kwak S, Hong SM, Lee JR, Takahara A, Seo Y. Nonisothermal crystallization behaviors of nanocomposites prepared by in situ polymerization of high-density polyethylene on multiwalled carbon nanotubes. Macromolecules. 2010;43(24):10545–53.

40. Wang SC, Zhang J, Chen SJ, Zhu H. Crystal structure and melting behavior of homo-polypropylene and heterophasic ethylene–propylene copolymer after long time heat treatment. J Cryst Growth. 2012;355(1):151–8.

41. Trujillo M, Arnal ML, Müller AJ, Laredo E, Bredeau S, Bonduel D, et al. Thermal and morphological characterization of nanocomposites prepared by in-situ polymerization of high-density polyethylene on carbon nanotubes. Macromolecules. 2007;40(17):6268–76.

42. Purohit PJ, Wang D-Y, Emmerling F, Thuenemann AF, Heinrich G, Schoenhals A. Arrangement of layered double hydroxide in a polyethylene matrix studied by a combination of complementary methods. Polymer. 2012;53(11):2245–54.